JOURNAL OF SPACECRAFT AND ROCKETS
Vol. 45, No. 1, January–February 2008

Analysis of the UNISAT-3 Solar Array In-Orbit Performance

Fabio Santoni*
University of Rome "La Sapienza," 00184 Rome, Italy
and
Fabrizio Piergentili†
University of Bologna, 47100 Forlì, Italy

DOI: 10.2514/1.32392

A technological experiment to assess the in-orbit performance of non-space-rated solar arrays is onboard the microsatellite UNISAT-3. These include terrestrial-technology monocrystalline silicon and low-efficiency triple-junction solar arrays, assembled using commercial off-the-shelf materials and following conventional non-space-rated procedures. A space-rated monocrystalline silicon solar array is also onboard, used for comparison of the achieved results. The manufacturing process is described and the solar array performance is evaluated based on the data collected in the first two-and-a-half years of operation in orbit. For both terrestrial-technology and low-efficiency triple-junction solar arrays, the observed solar array degradation is very fast in the first half-year, in which approximately one-fourth of the initial efficiency is lost. Then degradation stabilizes, showing a long-term decaying rate with a time constant of ten years, which makes the suggested technology suitable for small scientific and educational low-Earth-orbit spacecraft.

I. Introduction

THE microsatellite UNISAT-3, launched on a Dnepr launcher on 29 June 2004, is a university-class spacecraft, according to the definition given in [1], used as a testbed for commercial off-the-shelf (COTS) components in space [2,3]. It is based on the UNISAT microsatellite bus, developed following the philosophy of the Sapphire and Opal student-built satellites [4,5]. Use of COTS hardware in low-Earth-orbit spacecraft has been investigated by many authors. Results are available concerning electronic devices, propulsion systems, software, navigation, and payloads [6–10]. Use of COTS terrestrial Si solar arrays and COTS assembling materials for small-spacecraft photovoltaic systems was proposed in [11], motivated by the fact that spaced-rated solar arrays are typically very expensive in terms of specific cost (/W). Of course, there are other parameters describing the overall solar array performance, including specific power (W/kg), area power density (W/m^2), and stowage volume (W/m^3), which lead to a tradeoff between cost and performance at the spacecraft system level. In small scientific and educational spacecraft programs, typically facing strong economic budget restrictions, the specific cost is one of the main parameters to be considered, and because of economic budget limitations, use of expensive space-rated state-of-the-art hardware might not be practical. As far as solar arrays are concerned, according to [12], the specific cost of state-of-the-art triple-junction solar arrays can be estimated as 1000 /W, which is expected to be reduced four times using innovative technologies such as thin-film solar arrays. This is why in small scientific and education missions and, in particular, in university-class spacecraft, one can consider using less expensive, non-space-rated solar arrays, even if they perform less than state-of-the-art solar arrays. Literature is mainly devoted to state-of-the-art technologies, and rarely is information found concerning lesser-performing technologies. This is the main motivation for the technological experiment flown on the microsatellite UNISAT-3, developed to assess the in-orbit performance of two kinds of low-cost solar arrays: namely, inexpensive terrestrial-technology solar arrays, for which the cost can be evaluated as 20 /W at the beginning of life (BOL) and low-efficiency triple-junction (LETJ) solar arrays, assembled using commercial off-the-shelf materials and non-space-rated procedures, for which the cost is approximately 50 /W (BOL). Table 1 shows the main typical performance parameters of state-of-the-art, space-rated, triple-junction and thin-film solar panels, as given by [12,13], and the non-space-rated solar panels performance parameters, showing that these are competitive in terms of specific cost.

Technical feasibility of the use of terrestrial Si photovoltaic technology in low Earth orbit was evaluated in [11], in which the predicted operational lifetime was one year, based on conservative assumptions and by ground-test results. Prediction of the COTS solar array lifetime was not trivial, because of the lack of previous experience. The unknown behavior of solar cells' encapsulation materials, their space-radiation shielding effectiveness, and the potential degradation caused by the encapsulant yellowing in the strong UV radiation environment were the main aspects to be further investigated. The in-orbit experience after more than two-and-a-half years of operation in low Earth orbit shows that the initial prediction of one year was, in fact, pessimistic.

Recently, major photovoltaic companies began to manufacture and make commercially available triple-junction solar cells, delivered as a semifinite product, the cell-interconnect-coverglass (CIC) assembly, including a suitable coverglass and interconnectors, ready to be assembled in solar cell strings. The low-efficiency triple-junction solar cells are very attractive for small spacecraft. These are low-performance or defected solar cells, discarded by the space industry and therefore available at a reduced price. A procedure was set up to manufacture LETJ-based solar arrays in a conventional electronics laboratory, equipped with no professional solar array manufacturing devices and using COTS materials.

The UNISAT-3 photovoltaic system also includes a space-rated Si solar array, used as a reference to evaluate the results obtained for terrestrial Si and LETJ solar arrays. No significant degradation of the space-rated Si solar array was observed in the first two-and-a-half years of operation in orbit.

II. UNISAT-3 Photovoltaic System

The microsatellite UNISAT-3 has the shape of an octagonal prism: 16-cm width and 25-cm height. The solar arrays are mounted on the

Received 29 May 2007; revision received 22 August 2007; accepted for publication 15 October 2007.

*Associate Professor, Scuola di Ingegneria Aerospaziale, Dipartimento di Ingegneria Aerospaziale e Astronautica, Via Eudossiana 18.

†Assistant Professor, Dipartimento di Ingegneria delle Costruzioni Meccaniche Nucleari Aeronautiche e di Metallurgia, Group of Astrodynamics of the University of Rome.

Table 1 Solar array performance parameters

Solar array technology	Efficiency (typical)	Area power density, W/m^2	Specific power, W/kg	Specific cost, /W
Si (terrestrial)	14.8 %	180	23	20
LETJ	22.2%	275	70	50
Thin film	5–10%	80	250–500	250
Triple junction	28%	350	90	1000

Table 2 UNISAT-3 nominal solar array data

Solar array technology	I_{sc}, A (AM0,[a] room temperature)	V_{oc}, V (AM0,[a] room temperature)	Efficiency, %	Number of cells in series
Si (terrestrial)	0.43	13.3	14.8	24
Si (space-qualified)	0.42	13.2	15.0	23
LETJ (two parallel strings)	0.68	9.6	22.2	4

[a]AM0 is an acronym for air mass zero, indicating solar radiation power flux out of the Earth's atmosphere.

satellite external surface, one on each lateral face of the prism and two on each octagonal face. The photovoltaic system includes eight terrestrial-technology monocrystalline Si solar arrays, one space-qualified Si solar array, and three LETJ (InGaP/GaAs/Ge) solar arrays. Each solar array is directly connected to the battery through a blocking diode. In this configuration, the solar array voltage must be higher than the battery voltage (8.4 V nominal). Table 2 summarizes the UNISAT-3 solar arrays' technical data.

A. Silicon Terrestrial-Technology Solar Arrays

The UNISAT-3 terrestrial-technology solar arrays are based on high-efficiency monocrystalline Si solar cells, 20 mm × 60 mm in size, manufactured for terrestrial applications following the standards of commercial, non-space-rated, hardware. The solar array string includes 24 solar cells to fulfill the requirement of solar array voltage higher than the battery voltage. The solar array V_{oc} at room temperature is 13.3 V, and the temperature coefficient is approximately 55 mV/°C. A 24-series-connected solar cell string guarantees that the battery gets charged at solar array temperatures up to 80°C. The solar cells were screened on the basis of the I_{sc}, rather than on the usual maximum-power criterion, because the solar arrays work at a fixed voltage: namely, the battery voltage, lower than the maximum power voltage in nominal temperature conditions. In this voltage range, the solar cell performance is better described by the I_{sc}. The I_{sc} of the solar cell selected for flight is between 425 and 445 mA (435-mA mean value and 3-mA standard deviation). The low value of the standard deviation assures that all of the solar arrays have comparable efficiencies.

The solar panel's manufacturing process was developed on the basis of terrestrial application industrial standards, modified to make the system withstand the launch and space-environment loads, as described in detail in [11]. Si solar cell strings are laminated on aluminum perforated-honeycomb sandwich plates using the polymeric materials Tedlar® and ethylene vinyl acetate (EVA). A sandwich of EVA and Tedlar encapsulates the solar cell strings and the aluminum structural substrate, in which EVA is used as the bonding material, and Tedlar provides solar cell protection on the external surface and electrical insulation from the aluminum substrate on the internal surface, as shown in Fig. 1. This sandwich undergoes a lamination process in a vacuum bag, following a curing cycle during which the polymerization of EVA takes place. The EVA layer in contact with the aluminum is used to bond the solar array to the panel structure during the same curing process.

Fig. 1 Si terrestrial solar panel encapsulation and bonding on the structural substrate.

Terrestrial standard interconnections were used to build solar cell strings, soldered using the usual commercial electronics soldering equipment and materials.

The relation between the solar array short-circuit current and sun angle is shown in Fig. 2, in which the experimental data indicated by asterisks are compared with the theoretical cosine law (solid line). The deviation between the two is due to the effect of the encapsulant sunlight transmissivity.

B. Low-Efficiency Triple-Junction Solar Arrays

Three solar arrays installed onboard UNISAT-3 were manufactured using low-efficiency (22.2%) triple-junction solar cells (InGaP/GaAs/Ge), assembled using COTS industrial materials. The typical UNISAT-3 LETJ solar cell open-circuit voltage is 2.44 V at room temperature. Four solar cells are connected in series to reach the battery voltage, as required by the satellite power system architecture. It is well known that triple-junction solar arrays are less sensitive to temperature than Si solar arrays. However, a test campaign was performed to evaluate the temperature effects on the LETJ solar cells. The solar cell open-circuit voltage and short-circuit current density versus temperature are shown in Figs. 3 and 4. The resulting V_{oc} temperature coefficient is approximately 5.7 mV/°C, in close accordance with [14]. The solar array V_{oc} temperature coefficient is 22.8 mV/°C. The J_{sc} temperature coefficient is 0.012 mA/(cm^2 K), comparable with the results given in [15].

The solar arrays were integrated using commercial off-the-shelf materials and conventional soldering techniques. The triple-junction solar cell's CIC assembly is delivered with coverglass and two interconnectors already installed. This makes the solar cell's string-manufacturing procedure straightforward. The assembled strings

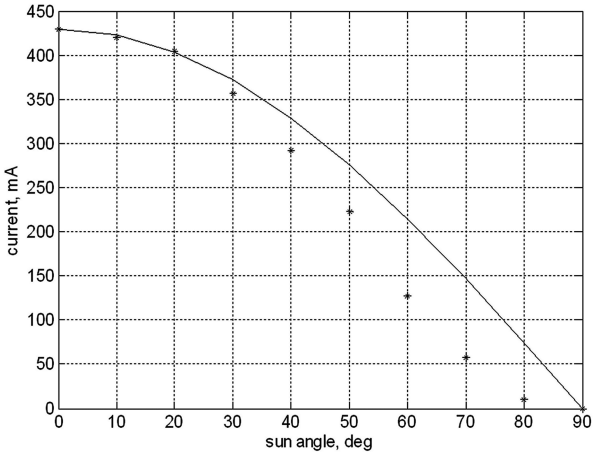

Fig. 2 UNISAT-3 measured solar array short-circuit current vs sun angle.

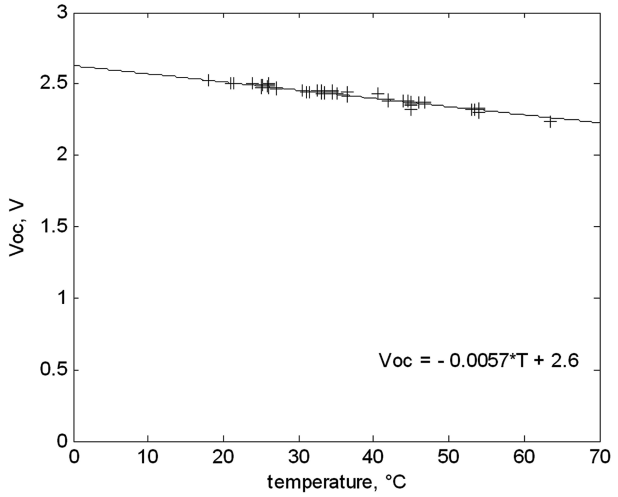

Fig. 3 UNISAT-3 low-efficiency triple-junction solar cells Voc versus temperature.

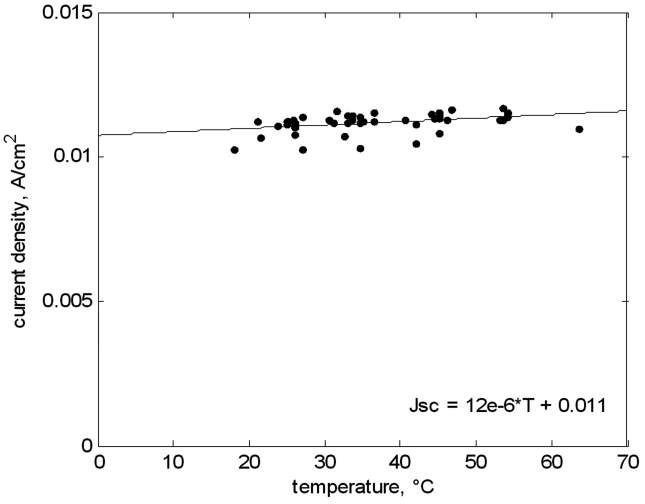

Fig. 4 UNISAT-3 LETJ solar cell short-circuit current density versus temperature.

were bonded on a fiberglass substrate using a commercial silicone rubber encapsulant for high-temperature terrestrial applications.

C. Space-Qualified Silicon Solar Arrays

A space-qualified Si solar array, assembled using high-efficiency monocrystalline space-qualified Si solar cells and space-rated assembling materials and procedures, was installed on UNISAT-3 and used to compare the results obtained for the non-space-rated solar arrays. Space-rated coverglasses were used for solar cell protection. The solar array consists of 23 solar cells connected in series, 15.0% nominal efficiency, 50×25 mm in size.

III. In–Orbit Performance

UNISAT-3 is in a sun-synchronous, slightly elliptical, orbit (710-km perigee and 790-km apogee). The spacecraft is stabilized using a passive magnetic attitude-stabilization system, including a permanent magnet aligned with the satellite axis of symmetry and hysteresis rods. The expected satellite-attitude motion is similar to an oscillating compass needle, providing two turns per orbit. The satellite's symmetry-axis oscillation amplitude with respect to the magnetic field is on the order of 10 deg. The rotation about the axis of symmetry is damped by the hysteresis rods, but it is not stabilized. Therefore, the top and bottom solar arrays' sun angles can be evaluated, assuming that they are approximately aligned with the Earth's magnetic field, whereas the lateral solar array sun angle varies in an almost-unpredictable fashion along the orbit. A coarse-attitude-determination system, based on a COTS three-axis magnetoresistive magnetometer (TAM), and sun measurements obtained by the solar array currents were included in the mission operation planning. However, due to the failure of one magnetometer channel, only two magnetic field readings are available. In addition, the Earth's magnetic field measurements are perturbed by the onboard permanent magnet's magnetic field, which can be considered as a constant bias, and by the magnetic hysteresis rod's magnetic field, which is very difficult to predict. An attitude-determination procedure was developed for this situation, as described in [16], reaching an accuracy of approximately 10 deg. This value is not accurate enough for solar array performance evaluation; this is why performance is evaluated based on direct measurements of the solar array current, with no reference to the satellite attitude. Because of the satellite-attitude motion, the solar arrays occasionally face the sun perpendicularly, registering a maximum of the current, which is assumed as the solar array's maximum deliverable current at that time.

The UNISAT-3 telemetry system downloads real-time measurements while the satellite is visible to the ground station. The maximum solar array currents registered during each passage are routinely stored in the ground station database. From these data, it is possible to get an estimate of the solar array performance. Usually, this is expressed in terms of efficiency, defined as the ratio between the solar array maximum deliverable power and incident light power. Onboard UNISAT-3, it is not possible to measure the maximum-power point, because the maximum current is measured at the battery voltage, which is not exactly the solar array maximum-power point, but very close. Within this approximation, the maximum current and efficiency performances are the same. Thus, we indicate $I_{\max}$ as the maximum current delivered at the battery voltage, and we select this as the parameter for solar array performance evaluation.

The three monitored solar arrays (namely, terrestrial-technology Si, LETJ, and space-qualified Si) are mutually orthogonal. When all three are in sunlight, the sun direction cosines, expressed in terms of the solar array currents, must respect the following geometrical constraint:

$$\sqrt{\left(\frac{I_{\mathrm{TSi}}}{I_{\max \mathrm{TSi}}}\right)^2+\left(\frac{I_{\mathrm{SQSi}}}{I_{\max \mathrm{SQSi}}}\right)^2+\left(\frac{I_{\mathrm{LETJ}}}{I_{\max \mathrm{LETJ}}}\right)^2}-1=0 \qquad (1)$$

This geometrical relation can be exploited in two ways. It can be used to validate instantaneous measurements and to get additional evaluations of the maximum solar array currents. The left-hand member of Eq. (1) is a measure of the deviation of the onboard measured sun unit vector norm from one, which can be used to validate single current measurements. Moreover, indicating N_s as the number of measurements for each passage in which all the three solar arrays are in the sun, the solar array maximum currents can be evaluated by minimizing the cost function

$$J=\sum_{k=1}^{N_s}\left[\sqrt{\left(\frac{I_{\mathrm{TSi}}^{(k)}}{I_{\max \mathrm{TSi}}}\right)^2+\left(\frac{I_{\mathrm{SQSi}}^{(k)}}{I_{\max \mathrm{SQSi}}}\right)^2+\left(\frac{I_{\mathrm{LETJ}}^{(k)}}{I_{\max \mathrm{LETJ}}}\right)^2}-1\right]^2 \qquad (2)$$

with respect to the maximum currents. In this way, estimates of the maximum currents can be obtained and compared with the direct measurements.

A. Terrestrial-Technology Si Solar Arrays

The terrestrial Si solar array lies on the satellite face aligned to the onboard magnetic dipole and it points to the Earth in the northern hemisphere. Therefore, during daylight passes over the midlatitude ground station at the University of Rome, the solar array is exposed mainly to the Earth albedo, not to the sun, whereas during night passes, it is in the eclipse in winter and in the sun for at least a portion of the pass in summer. This seasonal effect is evident in the measurements shown by dots in Fig. 5, in which maxima are reached at the summer solstice. Evaluations of the solar array maximum

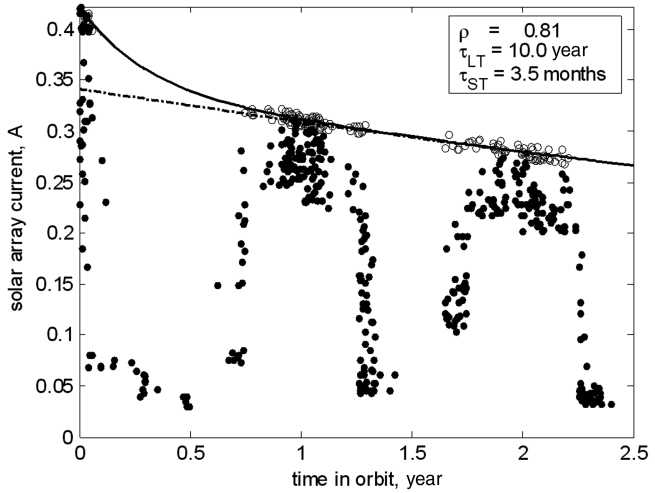

Fig. 5 UNISAT-3 terrestrial Si solar array maximum-current measurements (dots), evaluations (circles) and approximating curves (solid lines denote double-exponential and dotted lines denote long-term exponential).

currents were obtained using Eq. (2), assuming that the space-qualified Si solar array's maximum current is known and fixed, performing the minimization with respect to the terrestrial Si and LETJ solar array maximum currents. These are represented by circles in Fig. 5.

The degradation is very fast in the first period after launch and seems to stabilize after approximately six months. An approximating curve for the maxima can be expressed as the sum of two decaying exponentials, one at a long-term time constant t_{LT} and one at a short-term time constant τ_{ST}:

$$\frac{I_{\max}(t)}{I_{\max}(\mathrm{BOL})} = \rho e^{-t/\tau_{LT}} + (1-\rho)e^{-t/\tau_{ST}} \tag{3}$$

where $I_{\max}(\mathrm{BOL})$ is the maximum current at launch, ρ is the slow-decaying portion of $I_{\max}$, and the remaining part is the fast-decaying portion.

Data in Fig. 5 show that almost 29% of the initial efficiency is lost in the first year. Afterward, the efficiency decays slowly, with a ten-year time constant.

B. Low-Efficiency Triple-Junction Solar Arrays

The LETJ solar array maximum-current data are shown in Fig. 6, in which measurements are represented by dots and evaluations obtained by Eq. (2) are represented by circles. A lack of data is evident in the second quarter-year after launch. This is due to the fact that approximately three months after launch, the ground station was completely renovated to include automatic-operation hardware and software. In this period of time, for approximately two months, the satellite telemetry was downloaded approximately once a week. This reduced-operation regime is reflected in the amount of measured data, in which maximum currents are occasionally reached.

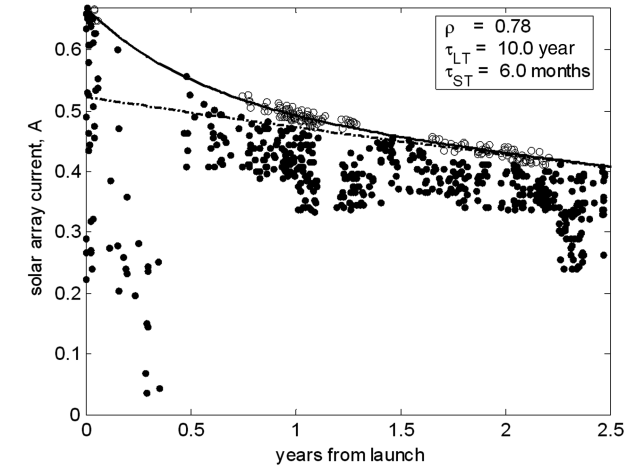

Fig. 6 UNISAT-3 low-efficiency triple-junction solar array maximum-current measurements (dots), evaluations (circles), and approximating curves (solid lines denote double-exponential and dotted lines denote long-term exponential).

As for the terrestrial Si solar arrays, the degradation is very fast in the first six months and stabilizes afterward. The maxima were interpolated by the sum of two decaying exponentials, as described by Eq. (3), with the values indicated in Fig. 6. In approximately three short-term time constants, 1.5 years, approximately one-third of the initial efficiency is lost. The slowly decaying curve has a ten-year time constant, identical to the terrestrial-technology solar arrays.

C. Space-Qualified Si Solar Arrays

The space-qualified Si solar array maximum-current data are shown in Fig. 7. No significant degradation of the solar array performance is registered. This can be used for a comparison with the other two technologies' performances.

D. Data Validation

The geometrical relation equation (1) was exploited to validate the raw maximum-current measurements. The values of Eq. (1) for all the measurements in which all three solar arrays are in the sun, obtained using the double-exponential curves for the maximum currents, are shown in Fig. 8. The mean error on the sun unit vector norm is approximately 1% and the standard deviation is slightly above 4%. This is due to environmental perturbations, mainly temperature and partial solar array shadowing by external satellite hardware, which are within the limits of the experiment setup.

IV. Discussion of In-Orbit Results

Surprisingly enough, the terrestrial-technology and LETJ solar arrays show a very similar degradation behavior. In particular, the presence of two time constants was not expected. In both cases, the short-term degradation time constant is on the order of the magnetic-attitude-stabilization system's time constant. However, the data of the space-qualified Si solar array, in which this time-dependent behavior is not observed, demonstrate that there is no correlation between the attitude stabilization and the maximum solar array measured current.

A. Terrestrial-Technology Si Solar Arrays

The terrestrial Si solar array degradation can be due to many environmental effects, including space radiation (mainly, protons in

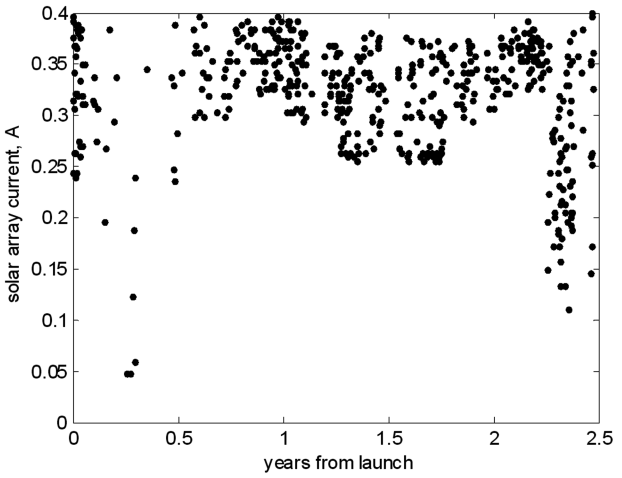

Fig. 7 UNISAT-3 Space-qualified Si solar array maximum-current measurements.

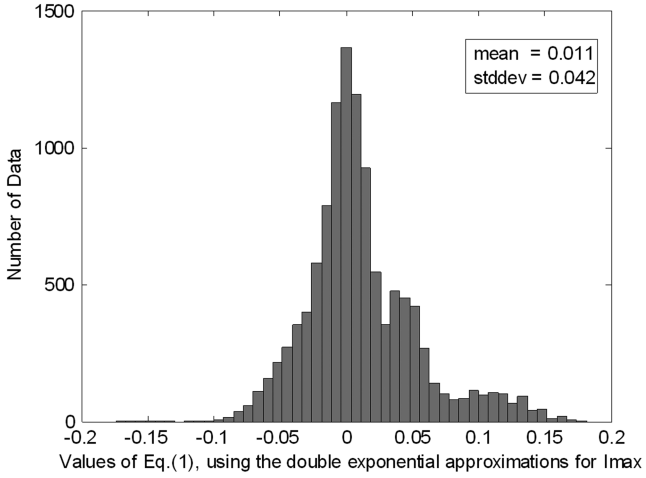

Fig. 8 Distribution of Eq. (1) values obtained by measurements and approximation (3) for Si and LETJ solar arrays.

the UNISAT-3 orbit), encapsulant yellowing due to the UV solar radiation, and increase in the solar array series resistance due to thermal cycling in orbit. The data available do not allow the distinguishing of the single-effect contribution. However, the last effect does not seem to concern the terrestrial Si solar array, because the series resistance influences the I–V curve mainly in the V_{oc} range, in which the UNISAT-3 terrestrial solar arrays do not operate.

Concerning the space-radiation effect, a worst-case estimate can be given, assuming that all the observed degradation is due to radiation. The protection offered by the polymeric encapsulants can be compared with that offered by a suitable coverglass of equivalent thickness. The degradation of a monocrystalline Si solar cell with different thicknesses of SiO_2 coverglass in the UNISAT-3 orbit is shown in Fig. 9, evaluated by numerical simulation using Solar Array Verification Analysis Tool (SAVANT) software [17]. In the same graph, the degradation curve of the terrestrial Si solar arrays, given by the approximating curve (3) is shown. It shows that the EVA–Tedlar sandwich protects the solar cells from proton-radiation effect as an equivalent SiO_2 coverglass between 2.5- and 5-μm thickness, which is approximately 50 times less than the coverglass thickness usually employed in space-qualified Si solar arrays.

B. Low-Efficiency Triple-Junction Solar Arrays

The space-radiation contribution to the LETJ array degradation in the UNISAT-3 orbit is mainly that of trapped protons, trapped electrons, and solar protons. The 1-MeV equivalent electron fluence was evaluated using the Space Environment Information System (SPENVIS) space-environment-simulation software [18]. For triple-junction solar cells, it is evaluated as 3×10^{-12} cm^{-2}, which is a very small value, making negligible contribution to the solar cell efficiency loss [19].

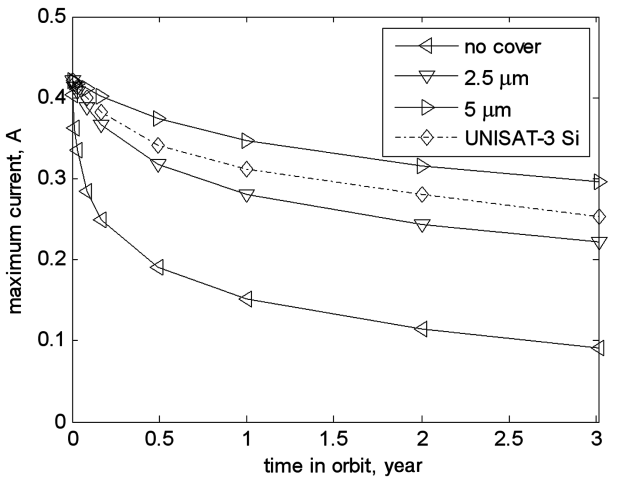

Fig. 9 Si solar array degradation for different coverglass thicknesses.

The LETJ solar array operates in a very-temperature-sensitive range of the solar array curve, and the performance may degrade significantly when the solar array gets too hot and the open-circuit voltage decreases, going down to the battery voltage. However, the temperature measurements in orbit show that the solar array operates well below the nominal reference temperature of 25°C, so that temperature cannot explain the LETJ solar array's maximum-current monotonically decreasing behavior observed in orbit.

The thermal cycling effect on the solar cell's interconnect solder joints was identified as the major cause of the triple-junction solar array efficiency loss. Thermal fatigue degrades the solder material's mechanical and electrical properties [20,21]. The solder joint's resistance contributes to the overall solar array series resistance modifying the solar array I–V curve slope at V_{oc}. The solar array fill factor decreases and the point of maximum power moves toward lower voltages. An experimental evaluation of the relation between solar array series resistance and thermal cycles is found in [22], in which results are given for 1000 cycles between −40 and 80°C and 20-min dwell time. This experimental setup reproduces the sun/eclipse times in orbit fairly closely, neglecting low-amplitude thermal cycles due to attitude motion. The relation obtained in [22] can be approximately summarized as 0.01% resistance change per thermal cycle, which, stated differently, indicates that the series resistance doubles every 10,000 cycles.

The silicone compound used to assemble the LETJ solar array is of commercial grade, not specifically intended for space use. This may have limited the interconnect thermal-stress-relief zone. In fact, the satellite was not expected to reach a very low temperature, but we actually found out that the solar arrays reach temperatures as low as −45°C. The compound at that temperature might have experienced a glass transition, becoming very hard and thus impairing the strain-relief motion. This has been observed, for example, in [23].

The effect of the series-resistance increase on the LETJ solar array performance was evaluated using a simplified solar-cell equivalent circuit, described in Appendix A, in which the three junctions are represented by three solar cells connected in series. The solar array I–V curve is given by

$$V = n_S \frac{kT}{q} \ell_n \frac{(I_{\text{phGe}} - I)^{A_{\text{Ge}}} (I_{\text{phGaAs}} - I)^{A_{\text{GaAs}}} (I_{\text{phInGaP}} - I)^{A_{\text{InGaP}}}}{I_{0_{\text{Ge}}}^{A_{\text{Ge}}} I_{0_{\text{GaAs}}}^{A_{\text{GaAs}}} I_{0_{\text{InGaP}}}^{A_{\text{InGaP}}}} - R_S I \tag{4}$$

where V is the solar array voltage, I is the solar array current, n_s is the number of solar cells connected in series, k is the Boltzmann constant, T is the temperature in Kelvin, q is the electron charge, I_{phi} is the ith-junction photocurrent, I_{0i} is the ith-junction reverse-saturation current, A_i is the ith-junction ideality factor, and R_S is the solar array series resistance. Numerical values are in Appendix A.

The UNISAT-3 solar array's working point is set by the battery voltage. The LETJ solar array's I–V curve obtained by Eq. (4) is shown in Fig. 10 for different values of R_S, showing that the current delivered by the solar array at battery voltage depends strongly on the series resistance and the battery voltage itself, depending on the battery charge status. The relation between solar array series resistance and current, obtained by Eq. (4) for $V = V_b$, is depicted in Fig. 11 as a function of the solar array series resistance, including the single effects of battery voltage and temperature, as well as their combined effects. It is evident that this relation depends strongly on temperature and battery voltage, and one cannot expect to obtain a measure of the resistance variation in orbit from the gathered maximum-current data. Nonetheless, temperature and battery voltage span approximately a fixed range and, assuming there is no solar array series-resistance variation, the maximum current should also span over a fixed range, occasionally reaching its maximum-possible value. In contrast, the maximum-current measurements and

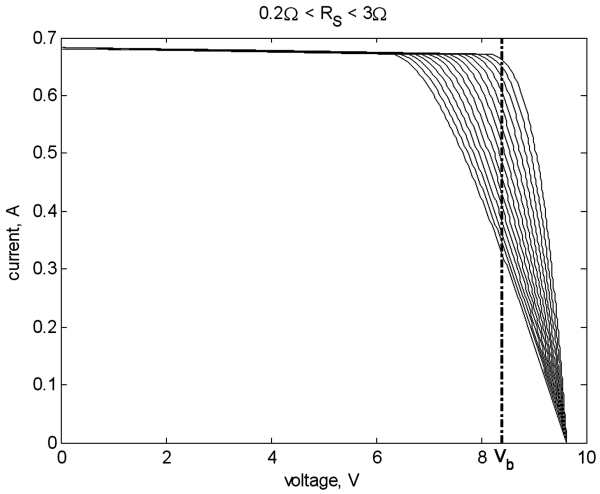

Fig. 10 LETJ solar array I-V curve for different series resistance (V_b is the battery voltage).

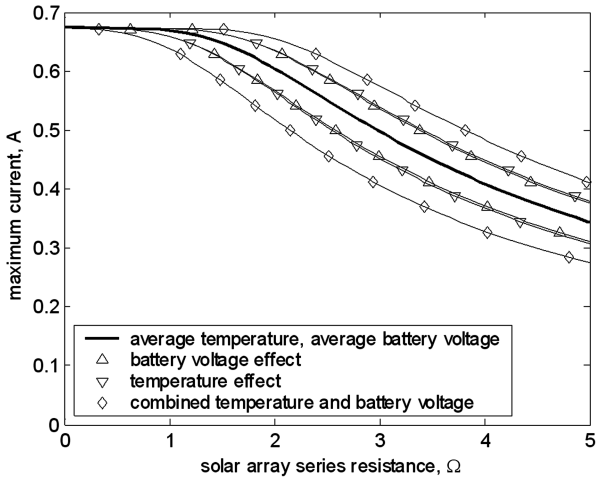

Fig. 11 LETJ solar array delivered current vs solar array series resistance.

evaluations show that the maximum solar array current follows a monotonically decreasing curve, which can be explained by the solar array series-resistance increment.

The observed maximum-current behavior suggests that additional effort must be put into the solar array assembly procedure, paying attention to insuring that the appropriate strain-relief margin is left for the interconnectors, avoiding any constrictions by the non-space-rated silicone compound. This is expected to improve the solar array behavior significantly, but it can be confirmed only by further ground or in-orbit testing. In any case, the effects of the series-resistance increment can be easily avoided by oversizing the solar array, making the open-circuit voltage sufficiently higher than the battery voltage. Adding one solar cell to the series-connected string increases the voltage margin by approximately 2.4 V, which is sufficient to avoid all of the temperature, battery charge, and series-resistance effects, at the expense of the increased solar array surface and cost.

C. Space-Qualified Si Solar Arrays

The measurement results in Fig. 7 show that space-qualified Si solar arrays have no significant degradation. This was indeed expected, because the space-radiation damage for space-qualified solar cells in the UNISAT-3 orbit is negligible.

D. Design Tradeoff

The tradeoff among different solar array technology depends on the system requirements and the mission's economic budget. Between the UNISAT-3 non-space-rated solar array implementations, the terrestrial Si solar arrays are the cheapest, in terms of cost per watt, but require a larger solar array area. According to the results obtained in orbit, the fast degradation in the first year of operation must be accounted for in the evaluation of end-of-life (EOL) performance, increasing the solar array area further. The LETJ solar arrays also show a fast degradation, but in contrast to the terrestrial grade Si, the assembling procedure has improvement margins and, in any case, the degradation effects can be avoided in a straightforward way, adding solar cells in series to the string, with minor impact on the system design and the assembling process. The cost is higher than for the terrestrial solar array, but still affordable for many university spacecraft budgets. The UNISAT-3 experience is that the LETJ solar arrays offer the best tradeoff for the typical requirements of small spacecraft and university-class spacecraft, allowing the photovoltaic system requirements to be affordably met.

V. Conclusions

The UNISAT-3 microsatellite photovoltaic system includes a technological experiment to assess the performance in orbit of non-space-rated solar arrays, including inexpensive terrestrial-technology Si solar arrays and low-efficiency triple-junction solar arrays, assembled using commercial off-the-shelf materials and non-space-rated procedures. These types of solar arrays are best suited for small scientific and education spacecraft, in which the specific cost per watt is often the most important solar array performance parameter. The results obtained in two-and-a-half years of UNISAT-3 solar array operation in orbit show that the non-space-rated solar array has a fast degradation in the first year, but it is much slower afterward, with a time constant of ten years. The terrestrial Si solar array degradation is mainly due to the encapsulation material yellowing and space-radiation effects, whereas the main cause of the low-efficiency triple-junction solar array degradation was identified in the thermal cycling effect on the solder joints, leading to a solar array series-resistance increment. The obvious conclusion is that the low-efficiency triple-junction solar array assembling process needs to be improved, paying particular attention to the solar cell interconnectors strain-relief motion. These improvements need to be validated by ground or in-orbit testing. However, a simple and safe way to avoid the series-resistance deleterious effects that showed up in orbit is to oversize the solar array voltage, with minor impact on the assembling process. The UNISAT-3 experience is that low-efficiency triple-junction solar arrays offer the best tradeoff for university-class-spacecraft system requirements, because, even if terrestrial Si solar arrays are much cheaper, a large surface may be necessary to meet the spacecraft power requirements.

Appendix A: Simplified Triple-Junction Solar Cell Mathematical Model

A simplified mathematical model of the triple-junction solar cell is obtained considering the three junctions represented by three solar-cell-equivalent circuits connected in series, as shown in Fig. A1.

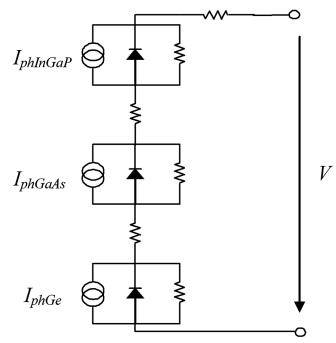

Fig. A1 Triple-junction solar cell simplified equivalent circuit.

Each solar cell junction is described by the equation

$$V_J = \frac{kTA_J}{q}\ell_n\left(\frac{I_{\mathrm{ph}J} - I}{I_{0J}} + 1\right) \tag{A1}$$

where V_J is the junction voltage, A_J is the junction diode-ideality factor, $I_{\mathrm{ph}J}$ is the junction photogenerated current, and I_{0J} is the junction reverse-saturation current. Series connection leads to

$$V = \frac{kT}{q}\left[A_{\mathrm{Ge}}\,\ell_n\left(\frac{I_{\mathrm{phGe}} - I}{I_{0\mathrm{Ge}}} + 1\right) + A_{\mathrm{GaAs}}\,\ell_n\left(\frac{I_{\mathrm{phGaAs}} - I}{I_{0\mathrm{GaAs}}} + 1\right) + A_{\mathrm{InGaP}}\,\ell_n\left(\frac{I_{\mathrm{phInGaP}} - I}{I_{0\mathrm{InGaP}}} + 1\right)\right] - R_s I \tag{A2}$$

where the junctions are named by the material, with evident meaning of the symbols. The reverse-saturation current density and ideality factor are set to $J_{0\mathrm{Ge}} = 10^{-6}$ A/cm^2, $A_{\mathrm{Ge}} = 1.4$, $J_{0\mathrm{GaAs}} = 510^{-12}$ A/cm^2, $A_{\mathrm{GaAs}} = 1.5$, $J_{0\mathrm{GaInP}} = 10^{-14}$ A/cm^2, and $A_{\mathrm{GaInP}} = 2$, according to [24]. The generation currents of InGaP, InGaAs, and Ge are set to 13.78, 15.74, and 20.60 mA/cm^2, respectively, according to [25].

Acknowledgments

The present work would not have been possible without the significant contribution of all the people, students, and professors directly or indirectly involved in the ten-year experience of the UNISAT program at the Scuola di Ingegneria Aerospaziale of the University of Rome "La Sapienza" and, in particular, F.Graziani. The authors wish to acknowledge the support of EniTecnologie (former Eurosolare) in the manufacturing of the UNISAT satellite's terrestrial solar array, and they are indebted to the Kiev Polytechnique Institute of the National Technical University of Ukraine for providing the UNISAT-3 space-qualified Si solar array. F. Santoni acknowledges the invaluable support received from R. J. Twiggs at Stanford University.

References

[1] Swartwout, M., "Twenty Plus Years of University-Class Spacecraft: A Review of What Was, an Understanding of What is, and a Look at What Should Be Next," 20th Annual AIAA/USU Conference on Small Satellites, Logan UT, Utah State Univ., Paper SSC06-I-314–17 Aug. 2006.

[2] Graziani, F., and Santoni, F., "The UNISAT Program for Space Education," 23rd International Symposium on Space Technology and Science, Matsue, Japan, Japan Society for Aeronautics and Space Science, Paper 2002-Keynote-03v, 26 May–2 June 2002.

[3] Santoni, F., Piergentili, F., Bulgarelli, F., and Graziani, F., "The UNISAT Program: Lessons Learned and Achieved Results," 57th International Astronautical Congress, Valencia, Spain, International Astronautical Congress, Paper 06-E1.1.10, 2–6 Oct. 2006.

[4] Swartwout, M., Kitts, C., and Cutler, J., "Sapphire: A Case Study for Student-Built Spacecraft," *Journal of Spacecraft and Rockets*, Vol. 43, No. 5, 2006, pp. 1136–1139. doi:10.2514/1.20465

[5] Twiggs, R. J., Cutler, J., Hutchins, G., and Williams, J., "Opal: A First-Generation Microsatellite Providing Picosat Communications for the Amateur Radio Community," 1999 AMSAT-NA Symposium, San Diego, CA, Radio Amateur Satellite Corp., North American Branch, Paper SSDL-99-20, Oct. 1999.

[6] Gibbon, D., Cowie, L., and Paul, M., "COTS (Commercial Off The Shelf) Propulsion Equipment for Low Cost Small Spacecraft," 38th AIAA/ASME/SAE/ASEE Joint Propulsion Conference and Exhibit, Indianapolis, IN, AIAA Paper 2002-3994, 7–10 July 2002.

[7] Adams, R. J., and Eslinger, S., "Lessons Learned from Using COTS Software on Space Systems," *Crosstalk: The Journal of Defense Software Engineering*, Ogden Air Logistics Center, Hill AFB, UT, June 2001.

[8] Goodman, J. L., "Lessons Learned From Flights of "Off the Shelf" Aviation Navigation Units on the Space Shuttle," *Joint Navigation Conference*, Joint Services Data Exchange, Los Angeles, 6–9 May 2002, pp. 1–16.

[9] Chau, S. N., Alkalai, L., and Tai, A. T., "Analysis of a Multi-Layer Fault-Tolerant COTS Architecture for Deep Space Missions," *3rd IEEE Symposium on Application-Specific Systems and Software Engineering Technology*, Inst. of Electrical and Electronics Engineers, Piscataway, NJ, 24–25 Mar. 2000, pp. 70–76.

[10] Underwood, C. I., and Oldfield, M. K., "Observed Radiation-Induced Degradation of Commercial-off-the-Shelf (COTS) Devices Operating in Low-Earth Orbit," *IEEE Transactions on Nuclear Science*, Vol. 45, No. 6, 1998, pp. 2737–2744. doi:10.1109/23.736522

[11] Agneni, A., Santoni, F., Ferrante, M., Romoli, A., and Ferrazza, F., "UNISAT Solar Array Integration And Testing," 5th International Symposium on Small Satellites Systems and Services, Centre National d'Etudes Spatiales, Paper S8.4, June 2000.

[12] Granata, J. E., Hausgen, P. E., Senft, D., Tlomak, P., and Merril, J., "AFRL Thin Film Solar Cell Development and Upcoming Flight Experiments," 2005 IEEE Aerospace Conference, Big Sky, MT, Inst. of Electrical and Electronics Engineers, Paper 1590, 5–12 Mar. 2005.

[13] Fatemi, N. S., Pollard, H. E., Hou, H. Q., and Sharps, P. R., "Solar Array Trades Between Very High Efficiency Multi-Junction and Si Space Solar Arrays," *28th IEEE Photovoltaic Specialists Conference*, Inst. of Electrical and Electronics Engineers, Piscataway, NJ, 15–22 Sept. 2000, pp. 1083–1086.

[14] Chiang, P. K., Ermer, J. H., Nishikawa, W. T., Krut, D. D., Joslin, D. E., Eldredge, J. W., Cavicchi, B. T., and Olson, J. M., "Experimental Results of GalnP2/GaAs/Ge Triple Junction Cell Development for Space Power Systems," *25th IEEE Photovoltaic Specialists Conference*, Inst. of Electrical and Electronics Engineers, Piscataway, NJ, 13–17 May 1996, pp. 183–186.

[15] Aiken, D., Stan, M., Murray, C., Sharps, P., Hills, J., and Clevenger, B., "Temperature Dependent Spectral Response Measurements for III–V Multi-Junction Solar Cells," *29th IEEE Photovoltaic Specialists Conference*, Inst. of Electrical and Electronics Engineers, Piscataway, NJ, 19–24 May 2002, pp. 828–831.

[16] Santoni, F., and Piergentili, F., "UNISAT-3 Attitude Determination Using Solar Panel and Magnetometer Data," 56th International Astronautical Congress, Fuluoka, Japan, International Astronautical Congress Paper O5-C1.2.06, 17–21 Oct. 2005.

[17] SAVANT, Solar Array Verification Analysis Tool, Software Package, Ver. 1.0.2. *NASA's Software Repository* [online database], http://technology.grc.nasa.gov/software/.

[18] *SPENVIS: The Space Environment Information System* [online database], http://www.spenvis.oma.be/spenvis/intro.html [retrieved Feb. 2007].

[19] Marvin, D. C., and Nocerino, J. C., "Evaluation Of Multijunction Solar Cell Performance in Radiation Environments," *28th IEEE Photovoltaic Specialists Conference*, Inst. of Electrical and Electronics Engineers, Piscataway, NJ, 15–22 Sept. 2000, pp. 1102–1105.

[20] Thébaud, J.-M., Woirgard, E., Zardini, C., and Sommer, K.-H., "High Power IGBT Modules: Thermal Fatigue Resistance Evaluation of the Solder Joints," *International Workshop on Integrated Power Packaging, IWIPP 2000*, Inst. of Electrical and Electronics Engineers, Piscataway, NJ, 14–15 July 2000, pp. 79–83.

[21] Woodrow, T. A., "JCAA/JG-PP Lead-Fee Solder Project: −20°C to +80°C Thermal Cycle Test," SMTA International Conference, Rosemont, IL, Curran Associates, Inc., Red Hook, NY, 24–28 Sept. 2006.

[22] Cuddalorepatta, G., Dasgupta, A., Sealing, S., Moyer, J., Tolliver, T., and Loman, J., "Durability of Pb-Free Solder Connection Between Copper Interconnect Wire and Crystalline Silicon Solar Cells: Experimental Approach," *11th International Symposium on Advanced Packaging Materials: Processes, Properties and Interface*, Inst. of Electrical and Electronics Engineers, Piscataway, NJ, 15–17 Mar. 2006, pp. 16–21.

[23] Blake, I. N., "Lessons Learned About Fabrication of Space Solar Arrays from Thermal Cycle Failures," *25th IEEE Photovoltaic Specialists Conference*, Inst. of Electrical and Electronics Engineers, Piscataway, NJ, 13–17 May 1996, pp. 329–332.

[24] Reinhardt, K. C., Mayberry, C. S., Lewis, B. P., and Kreifels, T. L., "Multijunction Solar Cell Iso-Junction Dark Current Study," *28th IEEE Photovoltaic Specialists Conference*, Inst. of Electrical and Electronics Engineers, Piscataway, NJ, 15–22 Sept. 2000, pp. 1118–1121.

[25] Nishioka, K., Takamoto, T., Agui, T., Kaneiwa, M., Uraoka, Y., and Fuyuki, T., "Evaluation of InGaP/InGaAs/Ge Triple-Junction Solar Cell Under Concentrated Light by Simulation Program with Integrated Circuit Emphasis," *Japanese Journal of Applied Physics*, Vol. 43, No. 3, 2004, pp. 882–889. doi:10.1143/JJAP.43.882

A. Ketsdever
Associate Editor